WATER RESOURCES RESEARCH, VOL. 42, W12S03, doi:10.1029/2006WR004929, 2006

Quantifying colloid retention in partially saturated porous media

Yuniati Zevi,[1] Annette Dathe,[1] Bin Gao,[1] Brian K. Richards,[1] and Tammo S. Steenhuis[1]

Received 30 January 2006; revised 14 August 2006; accepted 1 November 2006; published 16 December 2006.

[1] The transport of colloid-contaminant complexes and colloid-sized pathogens through soil to groundwater is of concern. Visualization and quantification of pore-scale colloid behavior will enable better description and simulation of retention mechanisms at individual surfaces, in contrast to breakthrough curves which only provide an integrated signal. We tested two procedures for quantifying colloid movement and retention as observed in pore-scale image sequences. After initial testing with static images, three series of images of synthetic microbead suspensions passing through unsaturated sand were examined. The region procedure (implemented in ImageJ) and the Boolean procedure (implemented in KS400) yielded nearly identical results for initial test images and for total colloid-covered areas in three image series. Because of electronic noise resulting in pixel-level brightness fluctuations the Boolean procedure tended to underestimate attached colloid counts and conversely overestimate mobile colloid counts. The region procedure had a smaller overestimation error of attached colloids. Reliable quantification of colloid retention at pore scale can be used to improve current understanding on the transport mechanisms of colloids in unsaturated porous media. For example, attachment counts at individual air/water meniscus/solid interface were well described by Langmuir isotherms.

Citation: Zevi, Y., A. Dathe, B. Gao, B. K. Richards, and T. S. Steenhuis (2006), Quantifying colloid retention in partially saturated porous media, *Water Resour. Res.*, *42*, W12S03, doi:10.1029/2006WR004929.

1. Introduction

[2] Colloids are ubiquitous in soil and subsoil and may be composed of any of a range of organic or inorganic components, including microorganisms, humic substances, clay minerals and metal oxides [*McCarthy and Zachara*, 1989; *Ryan and Elimelech*, 1996]. Pathogenic biocolloids (bacteria, viruses, and protozoa) have been implicated in waterborne disease outbreaks in the United States [*Barwick et al.*, 2000; *Macler and Merkle*, 2000]. Natural organic matter and other colloidal-sized materials may form stable complexes [*McCarthy and Zachara*, 1989; *Ryan and Elimelech*, 1996] with various pollutants previously considered to have very limited mobility in the subsurface, including trace metals [*Grolimund et al.*, 1996; *Grolimund and Barmettler*, 2002; *Jordan et al.*, 1997; *Karathanasis*, 1999; *Camobreco et al.*, 1996; *Richards et al.*, 1997, 1998, 2000; *McBride et al.*, 1997; *McBride*, 1998], pesticides [*de Jonge et al.*, 1998; *Sprague et al.*, 2000; *Williams et al.*, 2000] and radionuclides [*Smith and Degueldre*, 1993; *McCarthy*, 1998; *Kersting et al.*, 1999]. In a process termed colloid-mediated (or colloid-facilitated) transport, these complexes can significantly enhance the movement of contaminants in both saturated and unsaturated porous media.

[3] Colloid retention and mobilization in the unsaturated zone are not well understood. Breakthrough experiments allow quantification of colloid retention for various initial and boundary conditions, but they treat the system as a "black box" and cannot discriminate among the various retention mechanisms occurring within the column. Pore-scale visualization in unsaturated soils has been mainly limited to qualitative observations of colloid retention at various interfaces within the pore [*Chen and Flury*, 2005; *Sirivithayapakorn and Keller*, 2003; *Crist et al.*, 2004, 2005; *Zevi et al.*, 2005]. Quantitative determinations of colloid retention on a solid flat surface have only been carried out under saturated conditions [*Abdel-Fattah et al.*, 2001; *Elimelech et al.*, 2003; *Kuznar and Elimelech*, 2005] and it is not known whether these methods are applicable to unsaturated (i.e., partly saturated) conditions in actual porous media.

[4] Recently we used a confocal microscope to generate series of images [*Zevi et al.*, 2005] of colloid attachment at the air/water/solid interface (more accurately termed the air/water meniscus/solid (AW_mS) interface in that article) in a small flow chamber containing sand. These images qualitatively identified the retention mechanisms in unsaturated porous media. In that initial work, we did not attempt quantitative determinations of the retention mechanism(s), partly because few quantitative methods seemed to be available for analyzing images of colloid retention from digital and video microscopy. A subsequent look at image analysis technologies shows that biological and medical fields have made great advances in quantitative image analysis. Commercial image analysis packages available include Metamorph Imaging System, ImagePro, Clemex, PAX-it, AutoQuant, MCID, IQstudio and Zeiss Vision

[1]Department of Biological and Environmental Engineering, Cornell University, Ithaca, New York, USA.

0043-1397/06/2006WR004929$09.00

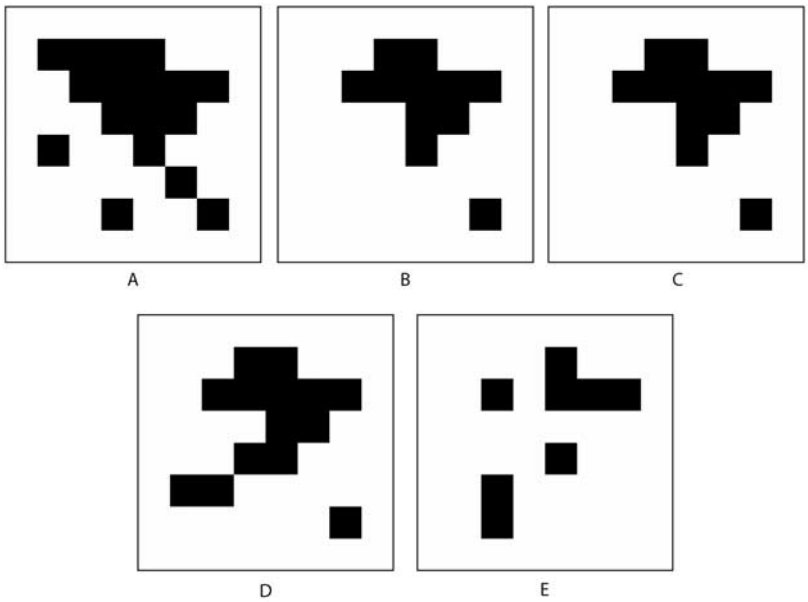

Figure 1. Five consecutive test images (each 8 × 8 pixels). All images are inverted so that colloidal particles appear as black.

KS400. Free public domain software is also available, such as Scion Image and ImageJ, both developed by the National Institutes of Health (NIH, http://rsb.info.nih.gov/nih-image/). These software packages can be adapted to count colloids attached at the AW_mS interfaces and thus quantitatively describe the colloid retention mechanisms in unsaturated porous media.

[5] Few applications exist which quantify transient processes, a capability that is needed for quantitatively evaluating colloid retention and release over time at the pore scale. In this paper, we developed and tested a colloid counting technique for a sequential stack of images where the numbers of mobile colloids (i.e., free in the water phase) and attached colloids (retained at the surface of sand grains) change in each image. This work builds on our earlier qualitative observations of colloid retention at the AW_mS interface which highlighted the need for quantification of transient colloid attachment and release in otherwise steady state water flux. Two of the most versatile visualization software packages were selected for testing: public domain ImageJ (NIH) and the high-end commercial KS400 (Zeiss Vision, Jena, Germany).

[6] On the basis of the work of *Sparks* [1987], *Aharoni et al.* [1991] wrote that "mechanistic meanings have been given to rate data solely on the fit of the data to an equation" and went on to state there is no guarantee that the best fit gives also the best physiochemical explanation. Although this was written in relation to adsorption of phosphorus, it applies equally well to colloid transport studies where the majority of the interpretation is still based on colloid breakthrough data. Only with accurate and quantitative pore-scale determination of individual mobile and attached colloids can realistic colloid retention mechanisms can be derived. This requires a reliable counting technique, making it essential that quantification procedures be tested and compared. The goals of this research were (1) to adapt existing still image methods to the quantification of transient colloid image sequences and (2) to compare the results generated by quantification procedures supported by the ImageJ and KS400 software packages when used for transient image analysis of colloid retention in actual porous media. Thus only with an accurate colloid quantification method is it possible to derive the governing mechanisms of colloid transport in subsurface environments, an approach currently not available for unsaturated soils. This paper meets this void.

2. Material and Methods

2.1. Colloid Imaging System

[7] A set of five consecutive test images was generated to compare the result of quantification process using the two software packages (Figure 1). Each image consisted of different numbers of white pixels in an 8 × 8 pixel array. Following this, three image sequences of colloid attachment in a small flow chamber (Figure 2) were used to test software performance with actual images. The visualization system consisted of a laser scanning confocal microscope, (Leica TCS SP2) with a HC PL APO CS 10.0 x objectives with a numerical aperture of 0.4, yielding a resolving power of 0.74 μm. The three image sequences were obtained from three experiments in which colloids were allowed to flow through a horizontal flow chamber under unsaturated conditions (Figure 3). The acrylic glass flow chamber (10 mm × 30 mm × 3 mm) had porous ceramic plates at the inlet and outlet to assure unsaturated flow conditions. A syringe pump supplied water at the inlet and a peristaltic pump removed the flow from the outlet. The chamber was filled with silica sand as specified below. Colloidal particles consisted of fluorescent synthetic carboxylated latex and polystyrene microspheres (Magsphere Inc, Pasadena, CA). As delivered, colloids contain surfactant with concentration of 3%, and we used 250x dilutions, thus yielding surfactant concentration of less than 0.01%. Nevertheless, in some cases we washed the colloids to remove the surfactant (by repeated rinsing with deionized water) because the presence

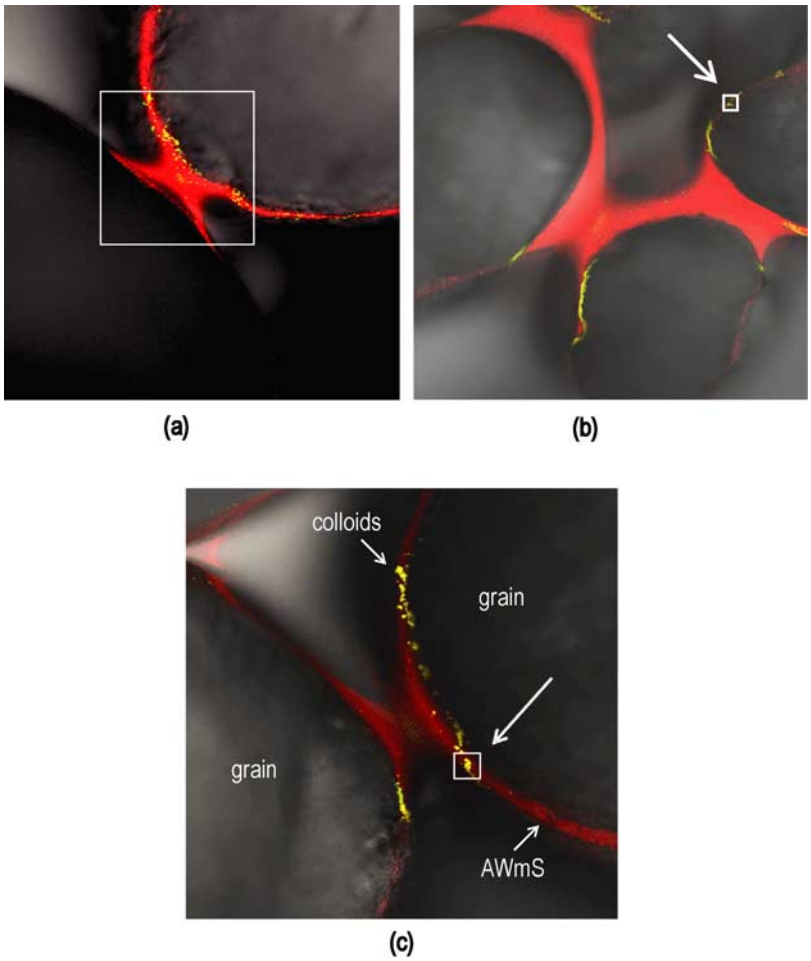

Figure 2. Three-channel overlaid confocal scanning laser microscope channel images from (a) series 1 (512 × 512 pixels, 748 × 748 μm), (b) series 2 (1024 × 1024 pixels, 748 × 748 μm), and (c) series 3 (512 × 512 pixels, 374 × 374 μm). The white rectangles in Figures 2a, 2b, and 2c are the locations of enlarged images shown as Figures 4, 7, and 8, respectively.

of surfactant may affect retention behavior at the AW_mS interfaces. The pH of the colloid suspension was 5.7.

[8] We chose images from widely varying experimental conditions for testing the quantification techniques (Table 1). Series 1 used coarse silica sand (average particle size 1.3 mm) and 1.1 μm unwashed carboxylated latex microspheres (1.4×10^8 particles/mL) at a suspension ionic strength that approached zero introduced at a flow rate of 0.15 mL/min (0.023 cm/s). In series 2 and 3 fine sand was used (average particle diameter 0.51 mm) with a suspension flow rate of 0.10 mL/min (0.015 cm/s). In series 2 the suspension was composed of 1.0 μm washed polystyrene microspheres (1.8×10^8 particles/mL) in a 1 mM NaCl solution. In series 3 the suspension was 1.0 μm unwashed polystyrene microspheres in a 200 mM NaCl solution. While the colloid addition was continuous in series 1 and 2, in the series 3 it was stopped at 8700 s after the onset of colloid additions. Additional experimental details of colloid solution preparation and operation of the microflow chamber are given by *Zevi et al.* [2005].

[9] The experimental conditions under which image sequences of pore-scale colloid behavior were taken are

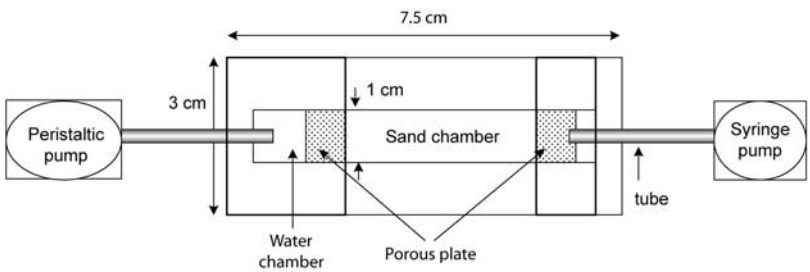

Figure 3. Schematic of the unsaturated sand flow chamber.

Table 1. Summary of Experimental Conditions

Experiment	Sand Texture	Colloid Type	Diameter, μm	Solution	Resolution, μm/pixel	Image Size, pixels	Time Step, s
Series 1	coarse	carboxylated (unwashed)	1.1	H_2O	1.46	512 × 512	2
Series 2	fine	polystyrene washed	1.0	1 mM NaCl	0.73	1024 × 1024	2
Series 3	fine	polystyrene unwashed	1.0	200mM NaCl	0.73	512 × 512	0.85

summarized in Table 1 and are available in the auxiliary material[1]. Series 1 had four separate image sequences. The first sequence contained only 21 frames (40 s long) followed by three sequences containing 61 frames each (120 s long each) taken successively. There were interruptions between sequences varying between 15 to 300 s, and the total elapsed time was 16 min. Series 2 had four more equally distributed sequences, each having 121 frames representing 240 s. With interruptions between sequences varying between 71 to 173 s, the total elapsed time was 40 min. Time steps between sequential images were 2 s for series 1 and 2. Series 3, a comprehensive view on colloid attachment over time at a single location, consisted of ten images sequences, each contained 61 frames (60 s long) except sequence 8 only 16 frames (25 s long), with intervals of about 1 hour between sequences 4 and 5 and between sequences 7 and 8, with an image time step of 0.85 s. Image sizes were 512 × 512 pixels for series 1 and 3, and 1024 × 1024 pixels for series 3. The resolution was 1.46 for series 1, corresponding to a frame area of 748 × 748 μm^2 and 0.73 μm/pixel for series 2 and 3, yielding frame areas of 748 × 748 μm^2 and 374 × 374 μm^2, respectively.

[10] The confocal microscope obtained separate images of the colloids, water and grains using three of five spectral channels available. In the first channel, emissions from the fluorescent colloids, excited at 488 nm using the argon laser, were recorded in the range of 500 to 540 nm. We used the same wavelength for both type of colloids. In the second channel, the water phase stained with Rhodamine B was excited at 543 nm using the green HeNe laser, with the emission recorded in the range of 555 to 650 nm. The concentration of Rhodamine B was very low (<0.001%) so as not to affect colloid behavior. The third channel detected transmitted light to show the location of the translucent silica sand grains. These three channels are here denoted argon, HeNe and transmitted light channel. Out-of-focus fluorescent light was removed by the Leica Confocal Software (LCS). The images acquired were 8 bit gray scale images; the argon and HeNe channels were false-colored green and red, respectively. An example of the confocal microscope output is given in Figure 4 showing images acquired for the three channels, taken from experimental series 1 sequence 4 (900 s after colloid solution application). Figure 4a shows the green colloids (argon channel), Figure 4b is the red water phase (HeNe channel), and Figure 4c depicts the two grains. The three channels are superimposed and shown as an overlay in Figure 2, where it is obvious that the colloids are entrapped in the region where the grain, water and air are in close proximity because the water menisci diminish to thin water films. We have thus named this region of colloid entrapment the AW_mS interface [*Zevi et al.*, 2005].

2.2. Image Analysis Software

[11] ImageJ is open source and flexible, and has been extended by the user community with both macros and plugins to accommodate all kinds of image processing. It has been used widely in biomedical applications such as counting nuclei [*Gering and Atkinson*, 2004], culture cell morphometry [*Prodanov et al.*, 2005] and measuring the thickness of an outer layer of bacteria [*Hope and Wilson*, 2003]. It has been used in soil science to determine material porosity from scanning electron microscope images [*Berryman and Blair*, 1986] and from computed tomography [*Moodley and Murrell*, 2004]. We are aware of no work reporting the use of ImageJ for quantifying colloid retention in unsaturated porous media. ImageJ has a feature that allows the user to easily define the region in which colloids will be counted. This region can be applied to all the sequential images in a stack, thus allowing automatic counting. Other commercial software packages offer this feature as well.

[12] KS400 is a high-end commercial software program package that is usually coupled with Zeiss microscopes and can control the microscope stage and camera. It can be operated independently on a PC using images obtained with any imaging system. User-defined macros can be coded easily and various available functions (for image enhancement, filtering, thresholding, and measuring) can be plugged into the user-specified code. KS400 is used widely in biology and medical sciences. For example, *Pernthaler et al.* [2003] developed an approach for automated counting of marine picoplankton stained with two fluorescent dyes. *Thiel and Blaut* [2005] developed a similar method for counting bacteria in human feces. In environmental sciences, the system has been used for obtaining fractal properties of porous media, especially soils [*Dathe et al.*, 2001; *Dathe and Baveye*, 2003; *Dathe and Thullner*, 2005]. For colloid research, KS400 has been used to determine the deposition rate of polystyrene particles [*Elimelech et al.*, 2003] and *Cryptosporidium* [*Kuznar and Elimelech*, 2005] onto micropatterned glass, from which the authors estimated the dimensionless Sherwood number. The Boolean procedure, which is available as a plugin function, compares two images and detects all pixels which appear at exactly the same position. Coded for consecutive images of a stack, it yields an easily implemented, computationally fast, reliable

[1] Auxiliary materials are available in the HTML. doi:10.1029/2006WR004929.

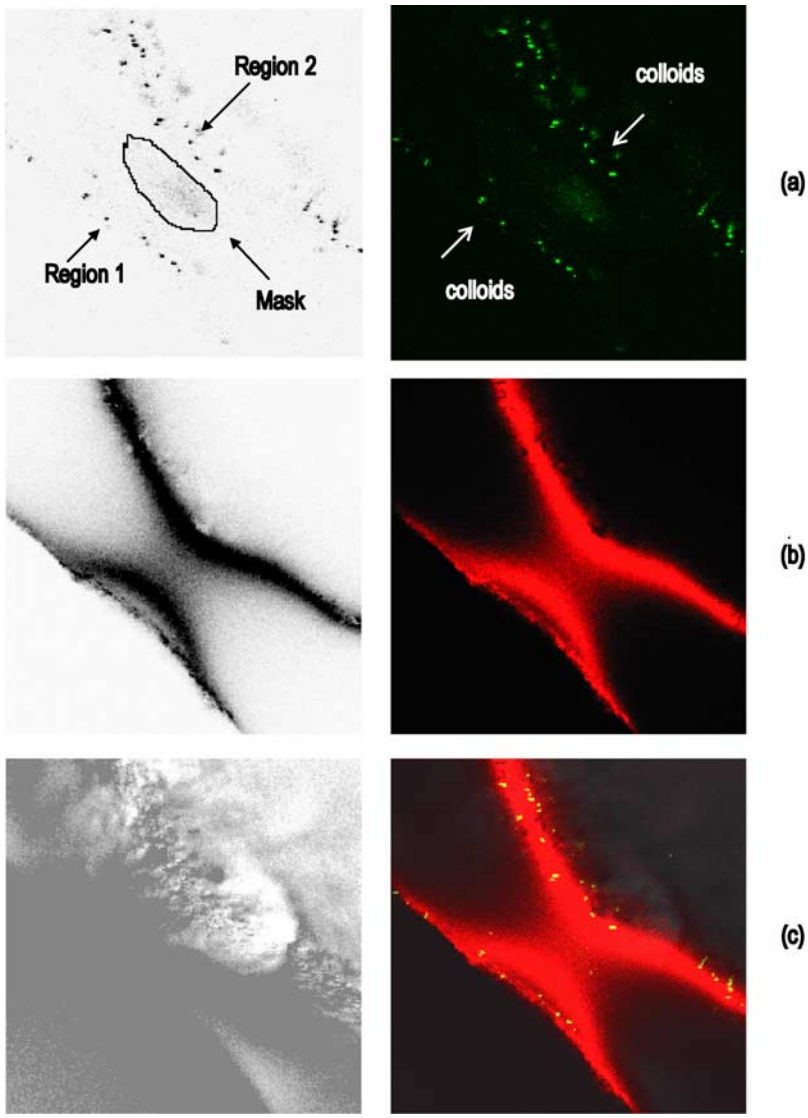

Figure 4. An example of confocal microscope image components enlarged from Figure 2a: (a) argon channel for detection of colloid fluorescence (inverted monochrome on left and false color on right). The image was divided into two regions for region procedure, with denoted area masked to avoid counting laser reflectance from the water surface. (b) HeNe channel for detection of water between grains including the menisci; images are inverted and false colored as in Figure 4a. (c) Sand grain locations shown by transmitted light channel (left) and overlay showing all three channels (right).

and repeatable procedure for detecting colloids which are attached to a grain surface.

2.3. Colloid Quantification

[13] To compare the quantification procedures, consistent image analysis techniques were used to transform the confocal microscope images to black and white (binary) images. These techniques consisted of taking the argon channel images (in which the colloid location information was stored), thresholding the images, separating pixels as either colloid or background, and selecting the region over which the counting will take place. No further image enhancement took place except where interference was encountered from spurious light reflecting from the water surface.

[14] In the thresholding process, gray values recorded by the argon channel ranging from 0 (black) to 256 (white), were separated by the gray value of 100. Pixels with a value of less than 100 were considered background (and colored black); those brighter were considered colloids and colored white. The value 100 was chosen empirically because the outline of colloids in thresholded images appeared the same as in the original images. This value of 100 also corresponded to the division between the continuous fluorescence spectra (indicating the background) and the discontinuous fluorescence spectra characteristic of the colloids.

[15] After thresholding the regions used for counting were chosen. The region selected differed for two "counting" procedures that were tested. In the first procedure for measuring the attached colloids, denoted as the region procedure, areas were selected near the AW_mS interface where the retention did or potentially could take place. In the series 1 and 3 cases, the region consisted of two separate

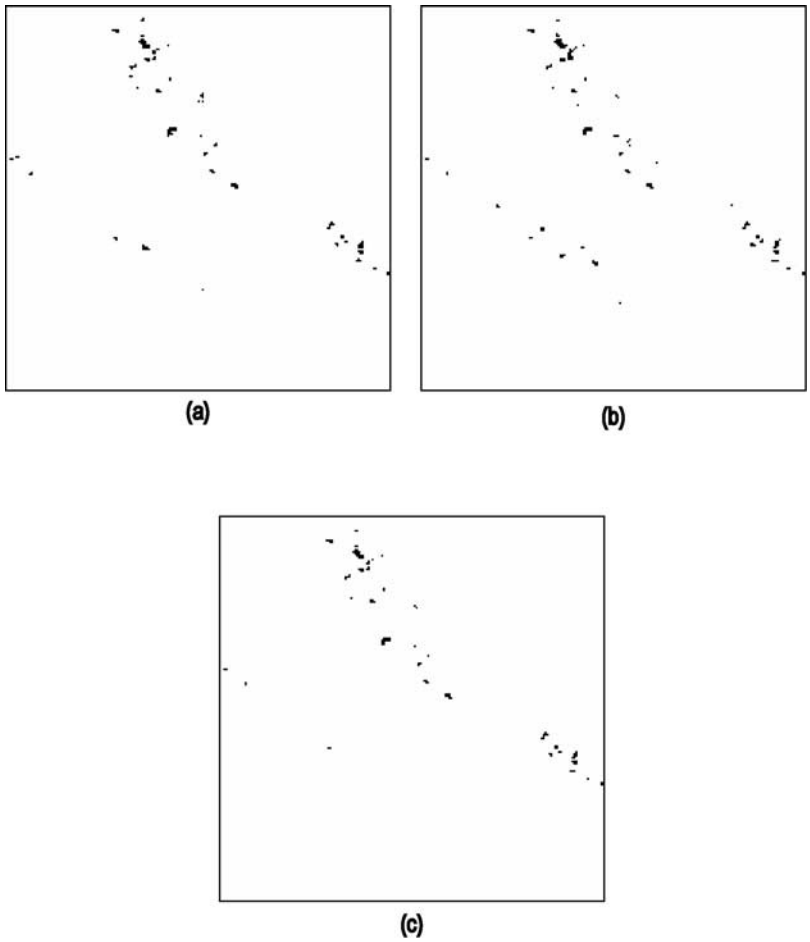

Figure 5. Boolean "and" operation: (a and b) two consecutive images with Δt = 1s and (c) pixel remaining at exactly the same position after performing the "and" operation.

areas at both sides of a pore between two grains. In series 2, four separate areas were selected because there were four grains with four AW_mS interfaces visible in the image. The selected areas for series 1 are shown in Figure 4a. This procedure was most easily applicable to the ImageJ software. For counting total colloids, the whole image (except the area covered with the mask) was selected as the counting region.

[16] For the second counting procedure, denoted as the Boolean procedure and most easily implemented with the KS400 software, the whole image was taken as the region, with the exception of a green spot representing the reflectance of laser light at the water surface, which appeared in series 1 and 2 and in the final three sequences of series 3. To avoid counting of these bright pixels as colloids, the green spot was masked with a black polygon. The exact location of the region and the mask selected for series 1 is shown in Figure 4a.

[17] In both counting methods, the numbers of white pixels in the selected regions were counted in each subsequent sequence. In the region procedure, pixels were counted as colloids when two or more pixels were connected using the eight-neighborhood method. It was not necessary for the colloids to remain at the same location; as long as they remained within the region they were counted as attached. In the Boolean procedure, two consecutive images were considered. Single white pixels that did not change between images were considered attached, whereas white pixels that were black in the consecutive image were thought to represent a moving, and hence suspended, colloid (Figure 5). The Boolean "and" operator in the software performed this comparison process automatically. Both the attached and total number of white pixels were counted for each image.

[18] The total area of colloids was then calculated as the product of the number of white pixels and the pixel size. The product was calculated within the measurement loop for the Boolean procedure, while for the region procedure it was calculated with a spreadsheet after all images in each sequence were counted.

3. Results

3.1. Test Images

[19] Five test images (depicted in Figure 1) were used to compare results generated by the region procedure (ImageJ software) and the Boolean procedure (KS400 software). The numbers of white pixels counted by both procedures are compared in Table 2. In test image A (Figure 1) 17 of the 64 pixels were white; as expected, both procedures identified 17 pixels as white. Similarly, the numbers of white pixels were counted correctly by both procedures for all

Table 2. White Pixel Counts in the Test Images of Figure 1 for the Region and Boolean Procedures[a]

Test Image	Region Procedure (ImageJ) Total of White Pixels	Boolean Procedure (KS400)	
		Total of White Pixels	White Pixels in Same Position
A	17	17	NA[b]
B	11	11	11
C	11	11	11
D	14	14	11
E	8	8	7

[a]The Boolean procedure also measures the number of white pixels that remain in the same position as in the preceding image.
[b]No prior image with which to compare.

other test images, as can easily be verified by the reader from Figure 1. The Boolean procedure also correctly determined the number of white pixels that remained in the same position in two consecutive images as can be seen, for example, by comparing the last two test images (D and E) in Figure 1. In test image D there were 14 white pixels and in test image E there were 8 white pixels, 7 of which were in the same position as in the preceding image. This is the value given in Table 2 for test image E.

3.2. Image Series

[20] In Figure 6 the colloid-covered areas are presented as a function of time following colloid application for the three image series. The areas measured on the y axis are normalized as the image fraction covered (colloid-covered area divided by the total image area). As we will see below, the total amount of colloids measured with the two approaches were nearly the same. However the assignment of colloids to the mobile versus attached categories varied greatly between the two counting procedures.

[21] In Figure 6 (top) the areas of mobile, attached and total colloids determined by both procedures are depicted for image series 1. Images were taken from 200 to 240 s and from 570 to 970 s. Figure 6 uses symbols to denote the classes of total, attached and mobile colloids, with blue indicating the region ImageJ results and orange the Boolean KS400 results. An interesting feature of this series is the sudden decrease in total and attached colloids at 665 s after colloid additions ceased. Close examination of the visible light channel (see also Animation S1 in the auxiliary material) showed that one of the grains shifted at that time point and subsequently returned to its original position at 720 s. Although this artifact would make the image unsuitable for quantifying colloid attachment processes in soil, it is useful for comparing the region and Boolean procedures.

[22] The greatest colloid-covered area measured was nearly 0.08 percent of the total area (with region procedure) at the end of the series 1 experiment, 16 min after initial colloid addition. Excluding the period when the sand grain moved (from 665 to 720 s), Figure 6 (top right) shows that the total colloid-covered areas increased in each interval and were nearly the same for both procedures, with the Boolean procedure yielding greater results (8.4%) than the region procedure. This is a consequence of the process that each procedure uses for considering what a colloid is: in the Boolean procedure each white pixel is assumed to represent a colloid, while in the region procedure, two white pixels that are connected are considered to be colloid. For this reason the differences between the two procedures are slightly greater during the initial phases of the experiment when there are fewer colloids and a relatively greater proportion of single colloids. The differences in the categorization of attached versus mobile colloids between the two procedures are much greater than the differences in total counts. Figure 6 (top left) shows that for the entire series 1 experiment, the Boolean procedure yielded a smaller count for attached colloids and hence (since mobile colloids are the difference between total and attached) a greater count for mobile colloids as compared with the region procedure.

[23] As noted previously, the sand grain movement at 665 s caused the measured attached area to decrease sharply, indicating that the number of attached colloids decreased, even after adjusting for the shifted location of the enumerated region. The detached colloids were mobilized, moving away with the flowing water out of the image field, explaining the delayed response of the mobile colloid counts. Although the magnitude of the response was different for the two procedures, both recorded the process well. From a mechanistic view, the phenomenon was interesting because it indicates that the colloids were not tightly attached to the grain/interface.

[24] For image series 2, the first images were taken at 935 s after adding colloids suspension. The interruptions in imaging were at 1180–1340 s and then two 80 s periods at 1650 and 1900 s. This experiment lasted nearly 45 min or 2.5 times longer than series 1. This was partly the cause of the greater retention of colloids than seen in series 1, with 0.4% of the total area occupied by colloids (with the region procedure) in series 2. As in series 1, this total colloid area was slightly greater for the Boolean procedure, with the differences again being the most pronounced at the beginning of the experiment. The categorization of attached and mobile colloids again showed a difference between procedures, with the Boolean procedure indicating 11 times greater fraction of mobile colloids.

[25] Series 3 was the longest experimental run with a total duration of 9115 s. Results were again similar to prior series: the region procedure yielded a slightly lower total colloid area count and a much greater area of attached colloids than the Boolean procedure. The mean areas of attached colloids in the last sequence of series 3 were 0.318 and 0.266% for the region and Boolean procedures respectively, similar to series 2 results despite a much longer duration. Figure 6 (bottom left) also shows that the colloid-covered area began to decrease slightly (12.2%) after colloid introduction ceased at 8700 s followed by adding a free of colloids solution.

4. Discussion

4.1. Comparison of Quantification Techniques

[26] In assessing the performance of the quantification approaches, it must first be remembered that the region and Boolean procedures were implemented with different software packages (ImageJ and KS400, respectively). If the quantification results had been identical (as we had hoped), it would have shown that both the software and procedure

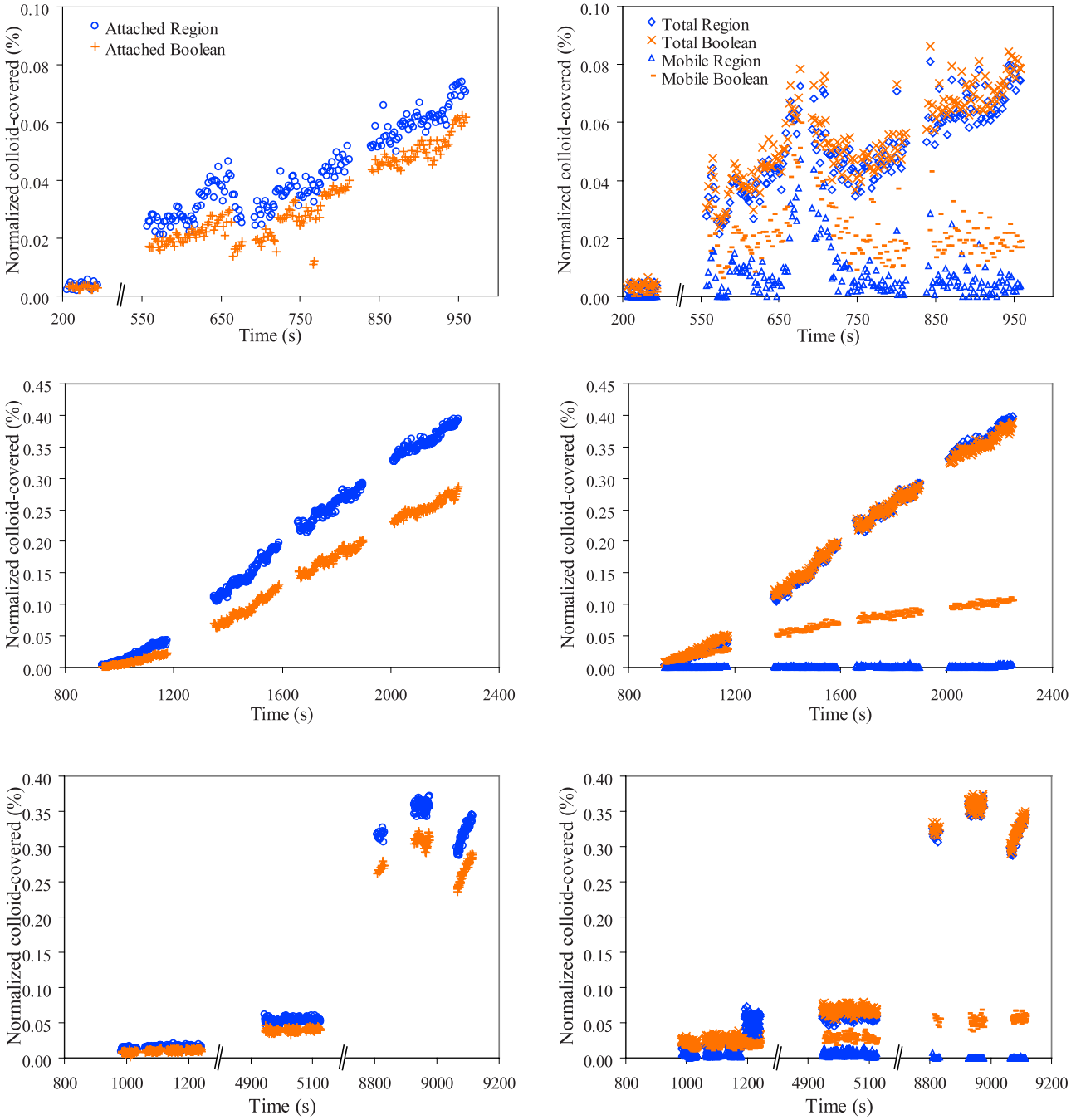

Figure 6. Colloid-covered areas as a function of time after the onset of colloid introduction for series (top) 1, (middle) 2, and (bottom) 3. Values on the y axis are expressed as colloid-covered fraction of the total image area.

could be used with the same precision. However, there were some differences in quantification, raising the question whether the sources of divergence were procedures (region versus Boolean) and/or the implementing software. To answer this question we first consider the results of the initial test images as well as the results for total colloid-covered area from the three experimental series. Table 2 shows that both approaches produced identical results for the initial test images. Similarly, determinations of the total colloid-covered areas in the experimental series were nearly identical between the two approaches (Figure 6) for all images examined. This is a good indication that the software packages were reporting reliable colloid coverage areas, which only requires counting white pixels in the whole image with no comparisons to other images in the time sequence. As indicated earlier, the slight differences in total colloid-covered area counts resulted from the procedural definition of what constituted a countable colloid. Unlike the Boolean, in the region procedure pixels were counted as colloids when two or more pixels were connected. Therefore to prove that both software packages are identical, we reran the ImageJ software without the

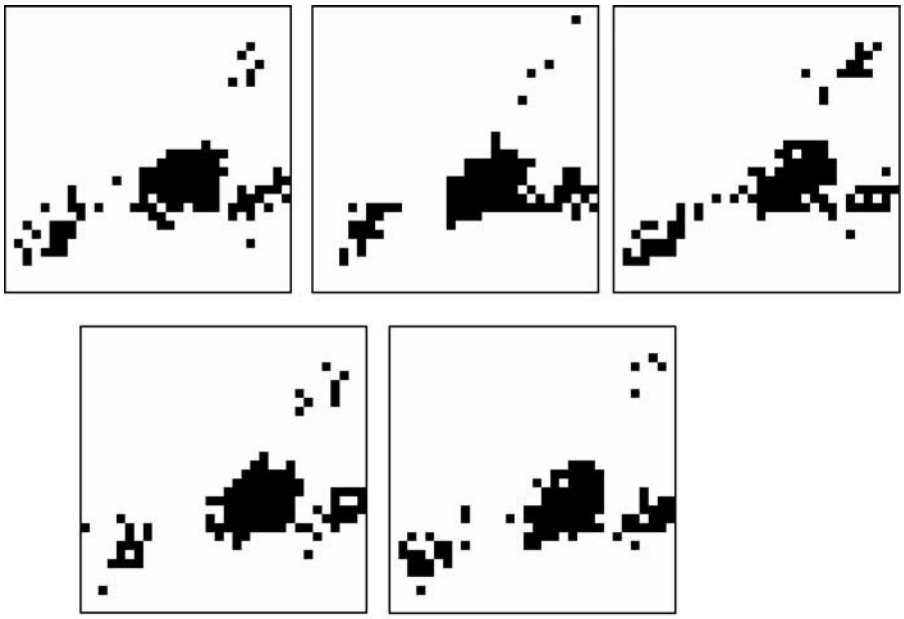

Figure 7. Detail of third sequence of series 2 around 1800 s (32 × 32 pixels or 23 × 23 μm, Δt = 2). The brightness of some attached colloids change in consecutive images, yielding lower attached colloid counts with the Boolean procedure.

restriction that two connected white pixels had to be present to represent a colloid. We exactly obtained the identical results. We may thus conclude that the respective software packages performed identically, and that remaining differences in the counts of the mobile versus attached colloids in the experimental series were due the procedure (region versus Boolean) and not the implementing software.

[27] The determinations of attached versus mobile areas differed substantially between the procedures (Figure 6), with the Boolean procedure consistently indicating a greater proportion of mobile colloids and conversely lower attached colloids. Attached colloid determinations are discussed first, since mobile colloids were simply the difference between total and attached colloid counts. The differences in attached colloid area can be attributed to two possible factors: overestimation by the region procedure or underestimation by the Boolean procedure. We will argue that both factors contributed to the disparity, but the underestimation error in the Boolean procedure was much more significant. Series 2 is first considered to avoid the complications introduced by the sand grain that shifted during series 1.

[28] In order to demonstrate underestimation by the Boolean procedure during series 2, the region with attached colloids in Figure 6 is greatly enlarged from the upper right corner of Figure 2b, so that single pixels are visible for five consecutive frames starting at time 1840 s (Figure 7). Close examination of the image sequences in Figure 7 reveals that images of attached colloids show discernable changes in brightness. This change in brightness, or flickering, occurs primarily in low signal areas around single colloids, at the fringes of a grouping of colloids, or in places thought to be out-of-focus colloids. The actual cause is thought to be due to the combination of two factors: (1) a pixel space being only partially occupied by a colloid and thus prone to report an ''average value'' near the 100 threshold and (2) temporal variation in how said pixel is evaluated due to random electronic noise of the instrument [*Zucker and Price*, 2001]. The flickering thus appears to be random and two-tailed, with pixels with values just below 100 flickering up as well as those with values just above 100 flickering down. Another contributing factor may be variable refraction effects of the water films present, but observations of dry colloids confirm a lesser degree of flickering with no water films present.

[29] This flickering has disparate effects on counts made by the two procedures. Because the flickering has no perceived bias, the average value reported by the region procedure is nearly constant. However, flickering will disproportionately affect the counts made by the Boolean procedure because individual pixels are compared in consecutive images, as demonstrated in Figure 7. A single attached colloid flickering on, off and on (i.e., above and below the gray value threshold of 100) in three consecutive frames affects the Boolean count comparisons, causing the procedure to regard that colloid as mobile in the two counts made by comparisons among the three frames. The converse is also true for a pixel flickering ''on'' for a single frame. The net effect is thus to increase the relative counts of mobile colloids in the Boolean procedure. Interestingly, averaging the values of a given pixel over two or four sequential images prior to Boolean analysis markedly reduces this error. For example, for series 2, the determination of attached colloids increased from 0.173% when measured from single frames frame to 0.187% when two frames were first averaged prior to the Boolean procedure. Averaging four frames increased the area to 0.198%, but there was little additional effect from averaging over larger numbers of frames. The coefficient of variation for the measurements decreased from 0.096 (every frame) to 0.091 (two and four frames). This averaging procedure smoothes the effects of flicker and thus reduces the overestimation of the mobile fraction.

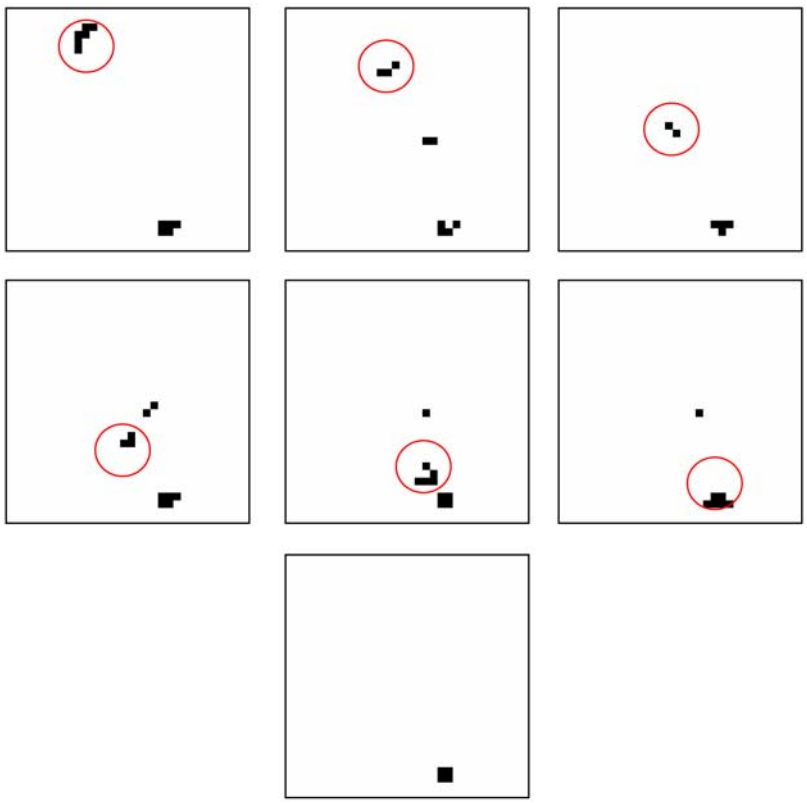

Figure 8. Detail of the series 3 sequence yielding the highest values for attached colloids around 9000 s (32 × 32 pixels or 23 × 23 μm, Δt = 0.85 s.). A colloid (circled) is moving very close to the AW_mS interface but does not attach. It is counted as attached when performing the region procedure.

[30] In a far less consequential error, the region procedure overestimates the attached colloid-covered area when mobile colloids move close to the interface but do not attach. This can be seen in close examination of an enlarged image sequence from series 3 starting at 5036 s, showing a spot at the lower part of the right grain (Figure 8). A colloid is moving through an area where colloids are already attached. In general, this overestimation is small, on the order of less than five percent.

[31] Additional interferences originated in the experimental setup, such as fluctuation in the meniscus position due to suction pulsations from the peristaltic pump at the outlet. This was especially notable in series 2 where the meniscus moved, as can be seen in Animations S1–S3. The shift in the sand grain during series 1 has already been noted, which had the effect of dislodging attached colloids as determined by both the region and Boolean procedures (Figure 6, top left). Even prior to the sand grain shift the data scatter was more notable for the series 1 experiment. Several factors contributed to this variability. The use of coarser sand and higher flow rate would tend to make colloidal attachments less stable. The coarser series 1 resolution (1.46 μm/pixel as compared to the better resolution of 0.74 μm/pixel in series 2 and 3) was coarser than the size of a single colloid, leading to the possibility of a single colloid being counted either once or twice, depending on whether it was straddling the boundary between two pixels, thus contributing another potential source of scatter.

[32] Counting the images using a mask reduced the total area of colloids. The mask, originally introduced to avoid the influence of spurious light, also obscured colloids moving through the masked area. This especially influenced the result when relatively few colloids were visible in the image. Masking should not influence the measurement of attached colloids, but does affect the estimation of mobile colloids as the difference between total and attached.

[33] Results were smoothest and most consistent in series 3. In terms of physical processes, this is not surprising in view of the greater solution ionic strength used, which strengthens colloidal attachment [*Saiers and Lenhart*, 2003]. Colloids were thus far more likely to remain in place, unlike the prior experiments conducted at much lower ionic strengths in which there was apparent subsequent movement of attached colloids. Data scatter, as reflected in the coefficient of variance in Table 3, also reflects this trend of greater stability correlating with greater ionic strength. (As previously noted, CVs also declined within each series as colloid numbers increased). This is a preliminary observation, but highlights the type of phenomenon that can be directly quantified with this approach.

4.2. Application of Quantification Techniques

[34] An application of the quantification approach presented here, showing how the results can be used to model colloid deposition on AW_mS interfaces. We assumed that the cumulative amount of colloids attached on the AW_mS interface in the image (M_s) is a function of the total amounts

Table 3. Coefficients of Variation for Boolean and Region Procedure Determinations of Total Colloid Counts in Three Experimental Series

	Coefficient of Variation	
Sequence	Boolean	Region
	Series 1	
1	0.178	0.284
2	0.180	0.207
3	0.254	0.187
4	0.107	0.140
	Series 2	
1	0.626	0.609
2	0.206	0.180
3	0.096	0.086
4	0.054	0.049
	Series 3	
1	0.204	0.195
2	0.134	0.169
3	0.145	0.165
4	0.116	0.140
5	0.059	0.074
6	0.053	0.066
7	0.038	0.048
8	0.019	0.016
9	0.020	0.021
10	0.055	0.051

of mobile colloids passing through (M_w) the image. As indicated, we are able to measure M_s directly through image analysis. The total amounts of mobile colloids passing through the image can be obtained by:

$$M_{w(i)} = M_{w(i-1)} + \frac{C_{w(i)} + C_{w(i-1)}}{2} \times \frac{v\Delta t}{L} \quad (1)$$

where $M_{w(i)}$ and $M_{w(i-1)}$ are the total amounts of colloids passing through image (i) and ($i - 1$) respectively, $C_{w(i)}$ and $C_{w(i-1)}$ are the amounts of unattached colloids in image (i) and ($i - 1$) respectively, v is the average velocity of colloids in the image, L is the average travel distance of colloids within the image, and Δt is time step between images (i) and ($i - 1$).

[35] The solid points in Figure 9 show the relationship between M_s and M_w for series 2 with Figure 9a showing the region procedure and Figure 9b showing the Boolean procedure. We used only this data set for this analysis because it is a continuous set of data, which are suitable for the calculations in equation (1). Also, as noted before, series 1 involved additional complications (i.e., the grain shift during the experiment). Although series 3 spanned a longer time than series 2, the measurements in series 3 were made at separate times (Figure 6, bottom).

[36] As expected, the relationships between M_S and M_w were different for the region and Boolean procedures. Figure 9 shows that the amounts of attached colloids (M_S) measured with region procedure were greater than the amounts measured with Boolean procedures. The differences between these two procedures were much greater for the total amounts of colloids passed through, where the M_w values of region procedure were about one tenth the values of Boolean procedure.

[37] In spite of the differences, the data from both the region and Boolean procedures can be described by the Langmuir equation:

$$M_s = \frac{KNM_w}{N + KM_w} \quad (2)$$

where K is the normalized adsorption rate constant (dimensionless), and N is the total available sites for colloid attachment at the AW_mS interface, with units of number of colloids. Figure 9 shows data and Langmuir model results. The best fitting K and N values for the region procedure were 3.61 and 14630 respectively. The best fitting parameters were much smaller for the Boolean procedure, with K of 0.29, and N of 4288. Although there were different values for parameters yielded by the two quantification procedures, which highlights the impact of method selection on results, the Langmuir model accurately describes the relationship between M_s and M_w for both procedures, with R^2 values greater than 0.98. This is not surprising, since the Langmuir concept is based on a fixed and limited number of attachment sites, which is valid for unsaturated soil at constant moisture content, which fixes the extent of air/water meniscus/solid interface available for attachment.

[38] The pore-scale quantifications can be used for qualitatively prediction of colloid movement at a larger scale. For example, the Langmuir relationship indicates that colloid retention at the AW_mS interface is not at a constant rate

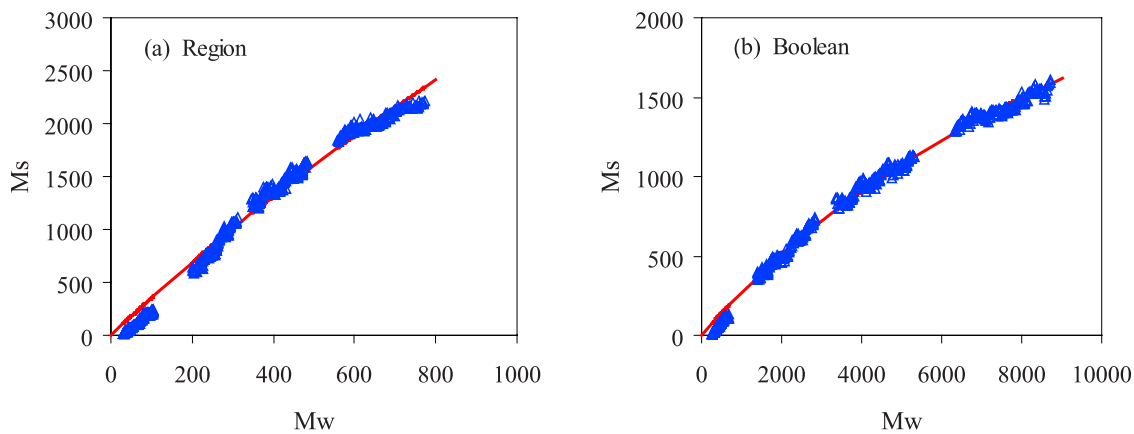

Figure 9. Langmuir $M_s - M_w$ relationships series 2 data determined with the region and Boolean procedures.

in the neighborhood of a grain as originally envisioned by *Yao et al.* [1971] for saturated porous media. It is of interest to apply the Langmuir model results to larger-scale events, e.g., column breakthrough curves, if the upscale method/theory was available. Because the parameters in the Langmuir equation are different for each interface, there remains a critical knowledge gap in quantifiably interpretation of pore-scale signals of all the interfaces.

[39] Further development of these quantification techniques are envisioned, including combining the region and Boolean procedures by first averaging successive frames (to reduce the electronic noise effects) and then dividing images into respective regions for attached colloids and the water phase. The area of attached colloids in each region could then be measured with the Boolean procedure, which would prevent erroneously counting (as ''attached'') mobile colloids moving across the region.

5. Conclusions

[40] Two procedures for quantifying colloid presence and retention in unsaturated sand were tested using ImageJ (implementing a region procedure) and KS400 (implementing a Boolean procedure). There was no difference in results between software packages when configured to the same colloid identification criteria. The region and Boolean procedures yielded identical results for test images and for total colloid counts in three series of experimental images, each series consisting of multiple experimental sequences. The two procedures diverged somewhat in mobile and attached colloid counts. The Boolean procedure tended to overestimate mobile colloid counts (and thereby underestimated attached colloid counts) due to electronic noise-induced flickering of pixels in areas of low signal strength (at edges of colloid groups, individual colloids, and out-of-focus colloids). The region procedure had a smaller overestimation error for attached colloid counts because mobile colloids passing through the counting region were regarded as attached.

[41] Overall, we showed that quantification procedures are feasible to form the basis for quantitative determination of colloid retention/mobilization mechanisms. For example, we showed in this work that attachment counts at the air/water meniscus/solid (AW_mS) interface were well described for both procedures by a Langmuir isotherm approach. Although further studies are needed to improve the accuracy of the quantification methods, this approach allows a better understanding and prediction of colloid transport behavior in unsaturated soil.

[42] **Acknowledgments.** The authors would like to acknowledge the capable assistance of Carol Bayles, manager of the Cornell Microscopy, Imaging and Fluorimetry Facility. This work was supported in part by the Cornell University Biocomplexity and Biogeochemistry Initiative.

References

Abdel-Fattah, A. I., M. S. El-Genk, and P. W. Reimus (2001), Automated video microscopic imaging and data acquisition system for colloid deposition measurements, *J. Colloid Interface Sci.*, *246*(2), 241–258.

Aharoni, C., D. L. Sparks, S. Levinson, and I. Ravina (1991), Kinetics of soil chemical reactions: Relationships between empirical equations and diffusion models, *Soil Sci. Soc. Am. J.*, *55*, 1307–1312.

Barwick, R. S., D. A. Levy, G. F. Craun, M. J. Beach, and R. L. Calderon (2000), Surveillance for waterborne-disease outbreaks—United States, 1997–1998, *MMWR CDC Surveillance Summaries*, *49*(ss-4), 1–35.

Berryman, J. G., and S. C. Blair (1986), Use of digital image analysis to estimate fluid permeability of porous materials: Application of two-point correlation functions, *J. Appl. Phys.*, *60*(6), 1930–1938.

Camobreco, V. J., B. K. Richards, T. S. Steenhuis, J. H. Peverly, and M. B. McBride (1996), Movement of heavy metals through undisturbed and homogenized soil columns, *Soil Sci.*, *161*(11), 740–750.

Chen, G., and M. Flury (2005), Retention of mineral colloid in unsaturated porous media as related to their surface properties, *Colloids Surf. A.*, *256*, 207–216.

Crist, J. T., J. F. McCarthy, Y. Zevi, P. C. Baveye, J. A. Throop, and T. S. Steenhuis (2004), Pore-scale visualization of colloid transport and retention in partly saturated porous media, *Vadose Zone J.*, *3*(2), 444–450.

Crist, J. T., Y. Zevi, J. F. McCarthy, J. A. Troop, and T. S. Steenhuis (2005), Transport and retention mechanisms of colloids in partially saturated porous media, *Vadose Zone J.*, *4*, 184–195.

Dathe, A., and P. Baveye (2003), Dependence of the surface fractal dimension of soil pores on image resolution and magnification, *Eur. J. Soil Sci.*, *54*(30), 453–466.

Dathe, A., and M. Thullner (2005), The relationship between fractal properties of solid matrix and pore space in porous media, *Geoderma*, *129*(3–4), 279–290.

Dathe, A., S. Eins, J. Niemeyer, and G. Gerold (2001), The surface fractal dimension of the soil-pore interface as measured by image analysis, *Geoderma*, *103*(1–2), 203–229.

de Jonge, H., O. H. Jacobsen, L. W. de Jonge, and P. Moldrup (1998), Particle facilitated transport of prochloraz in undisturbed sandy loam soil columns, *J. Environ. Qual.*, *27*(6), 1495–1503.

Elimelech, M., J. Y. Chen, and Z. A. Kuznar (2003), Particle deposition onto solid surface with micropatterned charge heterogeneity: The hydrodynamic bump effect, *Langmuir*, *19*, 6594–6597.

Gering, E., and C. T. Atkinson (2004), A rapid method for counting nucleated Erythrocytes on stained blood smears by digital image analysis, *J. Parasitol.*, *90*(4), 879–881.

Grolimund, D., and K. Barmettler (2002), Colloid-facilitated transport of pollutants: Phenomena and modeling, *Geochim. Cosmochim. Acta*, *66*(15A), A293–A293.

Grolimund, D., M. Borkovec, K. Barmettler, and H. Sticher (1996), Colloid-facilitated transport of strongly sorbing contaminants in natural porous media: A laboratory column study, *Environ. Sci. Technol.*, *30*(10), 3118–3123.

Hope, C. K., and M. Wilson (2003), Measuring the thickness of an outer layer of viable bacteria in an oral biofilm by viability mapping, *J. Microbiol. Methods*, *54*(3), 403–410.

Jordan, R. N., D. R. Yonge, and W. E. Hathhorn (1997), Enhanced mobility of Pb in the presence of dissolved natural organic matter, *J. Contam. Hydrol.*, *29*(1), 59–80.

Karathanasis, A. D. (1999), Subsurface migration of copper and zinc mediated by soil colloids, *Soil Sci. Soc. Am. J.*, *63*(4), 830–838.

Kersting, A. B., D. W. Efurd, D. L. Finnegan, D. J. Rokop, D. K. Smith, and J. L. Thompson (1999), Migration of plutonium in groundwater at the Nevada Test Site, *Nature*, *397*(6714), 56–59.

Kuznar, Z. A., and M. Elimelech (2005), Role of surface proteins in the deposition kinetics of *Chryptosporidium parvum* oocysts, *Langmuir*, *21*, 710–716.

Macler, B. A., and J. C. Merkle (2000), Current knowledge on groundwater microbial pathogens and their control, *J. Hydrol.*, *8*(1), 29–40.

McBride, M. B. (1998), Soluble trace metals in alkaline stabilized sludge products, *J. Environ. Qual.*, *27*, 578–584.

McBride, M. B., B. K. Richards, T. S. Steenhuis, J. H. Peverly, J. J. Russell, and S. Suave (1997), Mobility and solubility of toxic metals and nutrients in soil fifteen years after sludge application, *Soil Sci.*, *162*(7), 487–500.

McCarthy, J. F. (1998), Colloid-facilitated transport of contaminants in groundwater: Mobilization of transuranic radionuclides from disposal trenches by natural organic matter, *Phys. Chem. Earth*, *23*(2), 171–178.

McCarthy, J. F., and J. M. Zachara (1989), Subsurface transport of contaminants—Mobile colloids in the subsurface environment may alter the transport of contaminants, *Environ. Sci. Technol.*, *23*(5), 496–502.

Moodley, K., and H. Murrell (2004), A colour-map plugin for the open source, Java based, image processing package, ImageJ, *Comput. Geosci.*, *30*(6), 609–618.

Pernthaler, J., A. Pernthaler, and R. Amann (2003), Automated enumeration of groups of marine picoplankton after fluorescence in situ hybridization, *Appl. Environ. Microbiol.*, *69*(5), 2631–2637.

Prodanov, D., J. Heeroma, and E. Marani (2005), Automatic morphometry of synaptic boutons of cultured cells using granulometric analysis of digital images, *J. Neurosci. Methods*, *151*(2), 168–177.

Richards, B. K., T. S. Steenhuis, J. H. Peverly, and B. N. Liebowitz (1997), Effect of processing mode on trace elements in dewatered sludge products, *J. Environ. Qual.*, *26*, 782–788.

Richards, B. K., T. S. Steenhuis, and J. H. Peverly (1998), Metal mobility at an old, heavily loaded sludge application site, *Environ. Pollut.*, *99*, 365–377.

Richards, B. K., T. S. Steenhuis, J. H. Peverly, and M. B. McBride (2000), Effect of sludge-processing mode, soil texture and soil pH on metal mobility in undisturbed soil columns under accelerated loading, *Environ. Pollut.*, *109*, 327–346.

Ryan, J. N., and M. Elimelech (1996), Colloid mobilization and transport in groundwater, *Colloid Surf. A*, *107*, 1–56.

Saiers, J. E., and J. J. Lenhart (2003), Ionic-strength effects on colloid transport and interfacial reactions in partially saturated porous media, *Water Resour. Res.*, *39*(9), 1256, doi:10.1029/2002WR001887.

Sirivithayapakorn, S. S., and A. Keller (2003), Transport of colloids in unsaturated porous media: A pore-scale observation of processes during the dissolution of air-water interface, *Water Resour. Res.*, *39*(12), 1346, doi:10.1029/2003WR002487.

Smith, P. A., and C. Degueldre (1993), Colloid-facilitated transport of radionuclides through fractured media, *J. Contam. Hydrol.*, *13*(1/4), 143–166.

Sparks, D. L. (1987), Kinetics of soil processes: Past progress and future needs, in *Future Developments in Soil Science*, edited by L. L. Boersma, pp. 61–73, Soil Sci. Soc. of Am., Madison, Wis.

Sprague, L. A., J. S. Herman, G. M. Hornberger, and A. L. Mills (2000), Atrazine adsorption and colloid-facilitated transport through the unsaturated zone, *J. Environ. Qual.*, *29*(5), 1632–1641.

Thiel, R., and M. Blaut (2005), An improved method for the automated enumeration of fluorescently labelled bacteria in human feces, *J. Microbiol. Methods*, *61*, 369–379.

Williams, C. F., M. Agassi, J. Letey, W. J. Farmer, S. D. Nelson, and M. Ben-Hur (2000), Facilitated transport of napropamide by dissolved organic matter though soil columns, *Soil Sci. Soc. Am. J.*, *64*(2), 590–594.

Yao, K.-M., M. T. Habibian, and C. R. O'Melia (1971), Water and waste water infiltration: concepts and applications, *Environ. Sci. Technol.*, *5*(11), 1105–1112.

Zevi, Y., A. Dathe, J. F. McCarthy, B. K. Richards, and T. S. Steenhuis (2005), Distribution of colloid particles onto interfaces in partially saturated sand, *Environ. Sci. Technol.*, *39*(18), 7055–7064.

Zucker, R. M., and O. T. Price (2001), Statistical evaluation of confocal microscopy images, *Cytometry*, *44*, 295–308.

A. Dathe, B. Gao, B. K. Richards, T. S. Steenhuis, and Y. Zevi, Department of Biological and Environmental Engineering, Cornell University, Riley-Robb Hall, Ithaca, NY 14853, USA. (tss1@cornell.edu)